

# Avalanches Properties in a Self-Organized Critical Transport Model

GARCIA Luis and CARRERAS Benjamin A.<sup>1)</sup>

*Universidad Carlos III, 28911 Leganés, Madrid, Spain*

*1) Oak Ridge National Laboratory, Oak Ridge, Tennessee 37831-8070, U.S.A.*

*e-mail: lgarcia@fis.uc3m.es*

## Abstract

We have proposed a one-dimensional transport model based on critical-gradient fluctuation dynamics to describe some of the properties of plasma turbulence induced transport. This model has the characteristic properties of a self-organized critical (SOC) system. In this model, the flux is self-regulated by the stability properties of the fluctuations. A high-gradient edge region emerges where transport dynamics is close to marginal stability. The core remains at the subcritical gradient that is typical of a SOC system. Avalanches are quasi-periodic events triggered mostly near the edge region.

## Keywords:

SOC, avalanches, transport

## 1. Introduction

Self-organized criticality (SOC) dynamics [1] can explain some plasma transport phenomena that are difficult to explain with a purely diffusive transport model. Sandpile dynamics is an interesting paradigm for plasma transport [2, 3] and several models have been based on this analogy. We have proposed a one-dimensional transport model [4] that is a natural extension of the sandpile models applied to plasma transport. The model is based on critical-gradient fluctuation dynamics. It includes an evolution equation for the envelop of the plasma fluctuations and a transport equation with the diffusivity proportional to the fluctuation level. When the fluctuation evolution is introduced, fluctuation levels and fluxes of all magnitude are possible. We observed large fluctuation amplitudes propagating mostly inward and creating a wake of low-level stationary fluctuations. These low-level fluctuations cause a diffusion-like process while the large-level propagating fluctuations cause an avalanche-like transport. Here, we investigate the space-time structure of the avalanches. We show the existence of double quasi-periodic processes with well-defined space-time structures.

## 2. Model

The model proposed in Ref. [4] consists of two equations describing the evolution of the root-mean-square fluctuations,  $\Phi(x)$ , and of the averaged particle density,  $h(x)$ . They are

$$\frac{\partial \Phi}{\partial t} = \Phi(\gamma - \mu\Phi) + S_1, \quad (1)$$

$$\frac{\partial h}{\partial t} = \frac{\partial}{\partial x} \left( \mu_0 \Phi \frac{\partial h}{\partial x} \right) + S_0. \quad (2)$$

In the fluctuation equation,  $\gamma$  is the linear growth rate of the instability,  $\mu$  is the coefficient of the nonlinear term that is responsible for the saturation of the turbulence, and the third term,  $S_1$ , is a small source term to guarantee a minimal level of seed fluctuations. It is implemented as a low-level random noise that represents the trigger of a classical diffusion mechanism. The transport equation, Eq. (2), includes a radial diffusion term and a random source term,  $S_0$ . This source is implemented by the addition of an amount  $\delta$  with probability  $p_0 \Delta t / \delta$  each time step. In the diffusion term, we assume that the diffusivity is proportional to the level of fluctuations

and is given by  $\mu_0\Phi$ .

The underlying instability is assumed to be a critical-gradient instability. Then the linear growth rate is

$$\gamma = \gamma_0 \left( -\frac{\partial h}{\partial x} - Z_c \right) \Theta \left( -\frac{\partial h}{\partial x} - Z_c \right), \quad (3)$$

where  $\Theta$  is the Heaviside function, and  $Z_c$  is the absolute value of the critical gradient.

This model represents a generalization of the classical sandpile model used to interpret plasma transport [3] by the addition of fluctuation dynamics that regulates the amount of transport, which couples back to the fluctuations through the gradient drive.

The numerical scheme used in solving these equations is discussed in Ref. [4]. The boundary condition at the edge is  $h_{\text{edge}} = 0$  (open end). At the origin,  $h$  is time advanced by setting  $h_0^{t+\Delta t} = h_0^t - \Delta t \mu_0 \Phi_0^{t+\Delta t} Z_0$ . The fluctuation level  $\Phi$  is defined at radial points midway between grid points [4] so the values at the boundary do not enter in the scheme. For the results shown here,  $Z_c = 5$ ,  $\gamma_0 = 1$ ,  $\mu = 200$ ,  $\mu_0 = 100$ , and  $\Delta t = \delta = 0.05$ .

### 3. Description of the avalanches

Numerical results using the previously described model show first a transient phase followed by a steady state regime. In steady state, the function  $h$  can be characterized by its slope  $Z = -dh/dx$ . An example is shown in Fig. 1 for a system with size  $L = 3200$ . There are four well-defined regions. Near  $x=0$ , transport is dominated by slow diffusion caused by the background fluctuations, the  $S_1$  term in Eq. (1). In this region the profile is close to parabolic and  $Z$  is a linear function of  $x$ . There is also an edge pedestal region, for  $x > x_T$ , where  $Z$  is very close to the critical value and the transport is quasicontinuous. This transition point,  $x_T$ , depends on both  $p_0$  and the system size,  $L$ . The emergence of such pedestal and its properties was discussed in Ref. [4]. In the core, there are two regions. One has a nearly constant value for  $Z$  and remains subcritical. In this region, transport is dominated by intermittent avalanche-like events. Between this region and the edge pedestal there is a region with a linear increase in the slope. This suggests that diffusion may play a significant role in this region. We work within a range of parameter space where the profiles have a broad avalanche dominated region, and the jump in the slope stays just at the edge, as shown in Fig. 1.

In investigating the dynamics of this system, it is interesting to focus on the time evolution of the particle flux  $\Gamma = \Phi Z$ . There is a different dynamical behavior of the fluxes above and below the transition point,  $x_T$ . Between the transition point and the edge, there is continuous activity. In the inner region, there are quasi-periodic flux bursts which we call avalanches. They are the dominant transport mechanism. These avalanches are triggered in the outer region ( $x > x_T$ ), and they propagate inward ( $x < x_T$ ). They can penetrate all the way to the center of the pile. Few avalanches start in the inner region, but they are rare, and it takes a long time for them to build up. Although most avalanches propagate inward, all particle fluxes are positive, which causes outward transport of particles. If we look at the time trace of the fluxes at a fixed radial position  $x$ , the flux is bursty for  $x < x_T$ . It is practically zero most of the time, and suddenly a flux burst occurs. Above the transition radius, there is a continuous flux with what looks like a superimposed noise.

In Fig. 2, we have done a two-dimensional (2-D) plot of the contours of the flux. The plot shows eight major events in which the first avalanche reaches all the way to the center and every successive avalanche runs to a shorter distance inward. The inward penetration point of the avalanches appears to have a sawtooth-like envelope. We can see that most of the avalanches follow the pattern of having the termination point moving inwards after each avalanche. When the termination point of the avalanches has moved all the way to the edge

pedestal, a new avalanche goes all the way to the center and the process starts again. During an avalanche, the functional form of the flux at a given time is a front-like structure and it propagates inwards at a practically constant speed. Near the termination point, the flux propagation slows down. These properties are illustrated in Fig. 3, where we have plotted a sequence of radial profiles of the flux during an avalanche. The plots are done at equal time intervals. This front-like structure is driven by a supercritical value of  $Z$  at a single cell, just at the position of the front.

We have used the functional form of the avalanche as a way to identify them and determine their basic parameters. In a radial position where no avalanche is present, we follow the time evolution of the flux. The appearance of a maximum in the flux is an indication that an avalanche starts. We look at the evolution of its neighboring cells to determine the direction of propagation. Then we follow the evolution of the maximum of the flux as a way of tracking the avalanche. Parameter such as initiation point, penetration point, length, duration, and total flux can be determined in this way for each avalanche. These measurements allow us to study the statistical properties of the avalanches.

The distribution of initiation points of the avalanches and of the points of maximum inner penetration show clearly the qualitative features described in the previous section. An example of these distributions for  $L = 1600$  is shown in Fig. 4. We can see that most avalanches start at the boundary with the edge barrier region. They can penetrate all the way in and the probability of avalanches starting in the inner region decays exponentially inward relatively fast. The two regions in the PDF correspond to the two regions in the slope profile as can be seen in the figure.

We are interested in the avalanches that penetrate the core region. As shown in Fig. 5, the probability distribution function of the length and duration of these avalanches is practically flat. This is consistent with the detail evolution of the avalanches shown in Fig. 2.

#### 4. Quasi-periodic events

Let us consider with more detail the dynamical process of the avalanches. In Fig. 6, we have plotted the profile of the slope  $Z$  for  $L = 1600$ . In the figure, we compare the time-averaged profile with an instantaneous profile at a given time, excluding the avalanches. For the same time, we have plotted in Fig. 7 the instantaneous profile of  $\Phi$ .

We see that the instantaneous  $Z$  profile has a region with strong radial fluctuations in the inside and a relatively smooth profile outside. Both regions are separated by a deep minimum in  $Z$  at  $x = x_m$ . The reason for that is that the minimum is the point where most of the avalanches coming from the edge finish. The position  $x_m$  of the minimum moves outwards with time, it is what determines the edge of the sawtooth in Fig. 2. The functional dependence of  $x_m$  with  $t$  is practically linear.

In the inner region, there is no activity and  $\Phi$  remains very low. Therefore, diffusion is low and the spikes generated by the avalanches stopping are not eroded. In the outer region, the avalanches travel through, and they leave behind a tail of fluctuations that decays slowly as  $1/t$ . This fluctuation tail gives an average fluctuation level that enhances diffusion and causes the profile to be smooth.

When  $x_m$  reaches at its maximum value is set back to zero. As the minimum in  $Z$  moves outward it becomes shallower and some avalanches can go through all the way to  $x = 0$ . When they do so, they also smooth out the inner region. At the point that the whole core is smooth the avalanches penetrated all the way through and the process start again. The maximum value of  $x_m$  is about the position where the time averaged  $Z$  profile changes from being constant to increasing with radius.

The dominant avalanche processes in the region where the profile is smooth have a quasi-

periodic character. This quasi-periodicity of the avalanches is similar to the one observed in the diffusive sandpile for small values of the roughness of the profile [5]. The quasi-periodicity is evident in the power spectrum of the flux across a fixed radial position. An example of the spectrum is shown in Fig. 8 for  $L = 400$  at  $x = 200$ , in the avalanche dominated region. There are two clear peaks in the spectrum. The lowest frequency peak is associated with the frequency of the combined events like the ones shown in Fig. 2. The second peak corresponds to the frequency of the individual avalanches. For frequencies below this second peak, the spectrum shows the  $1/f$  decay characteristic of SOC systems.

An estimate of the frequency of the avalanches can be made by assuming that the transport at the core is totally dominated by these quasi-periodic events. The flux during a full event can be estimated by calculating the time behavior of the fluctuations triggered by one of the front-like events such as the ones in Fig. 3. After the event is been triggered,  $\gamma = 0$  in Eq. (1) and we can neglect the effect of the source over a short time equal to the period  $T$  between avalanches. Then, integrating Eq. (1), we obtain

$$\Phi(x, t) = \frac{\Phi_1}{1 + \mu\Phi_1 t}, \quad (4)$$

where  $\Phi_1$  is an integration constant. Then the flux balance at the transition point is approximately given by

$$p_0 x_T T_2 = \frac{\mu_0}{\mu} \langle Z \rangle \ln(1 + \mu\Phi_1 T_2). \quad (5)$$

Since  $x_T$  is close to  $L$ , the frequency of the avalanches, the second peak in the spectrum of Fig. 8, is a function of  $Lp_0$ . On the other hand, the frequency of the combined events, because there is a linear dependence on the penetration points must be proportional to the frequency of the avalanches divided by  $L$ . Therefore, the frequency of the combined events (first peak in the spectrum) is only a linear function of  $p_0$ . We have done a sequence of calculations varying  $L$  but keeping  $p_0 L = 0.016$  constant, where these properties of the frequencies of the two peaks of the flux spectrum have been confirmed.

## 5. Conclusions

For the range of parameter space considered in this paper, the transport model based on critical gradient fluctuation dynamics leads to results very similar to the sandpile with diffusion. The dynamics of this model is close to the sandpile dynamics when the roughness of the profile is slow. In this situation the profile is smoothed enough by the diffusion and avalanches became quasi-periodic events that are triggered near the edge of the system and penetrate inwards. Because the diffusive term is created by the wake of the avalanches, there is strong coupling between the size of the diffusion in a radial region and the frequency of the avalanches crossing that region. This leads to a double periodicity of the avalanches.

## References

- [1] P. Bak, C. Tang, and K. Wiesenfeld, *Phys. Rev. Lett.* **59**, 381 (1987).
- [2] P. H. Diamond, and T. S. Hahm, *Phys. Plasmas* **2**, 3640 (1995).
- [3] D. E. Newman, et al., *Phys. Plasmas* **3**, 1858 (1996).
- [4] L. Garcia, B. A. Carreras, D. E. Newman, *Phys. Plasmas* **9**, 841 (2002).
- [5] D. E. Newman, et al., *Phys. Rev. Lett.* **88**, 204304 (2002).

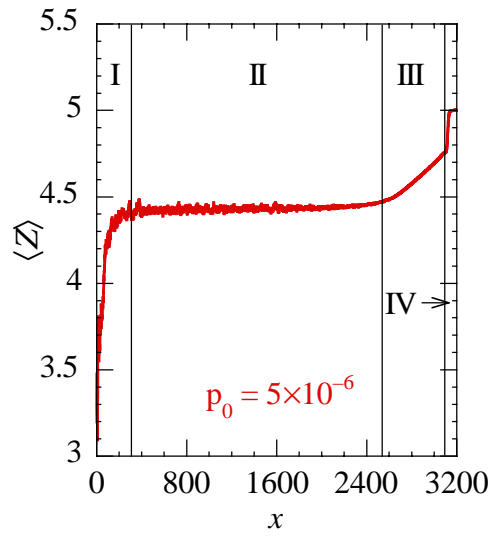


Fig.1 Time-averaged slope of  $h$ , showing the four characteristic transport regions.

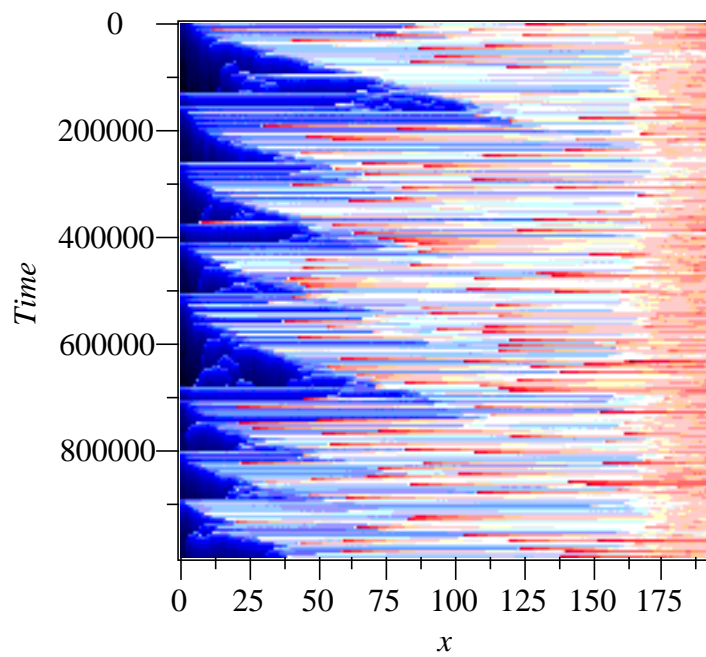


Fig.2 A 2-D plot of the contours of the flux in the time-radius plane.

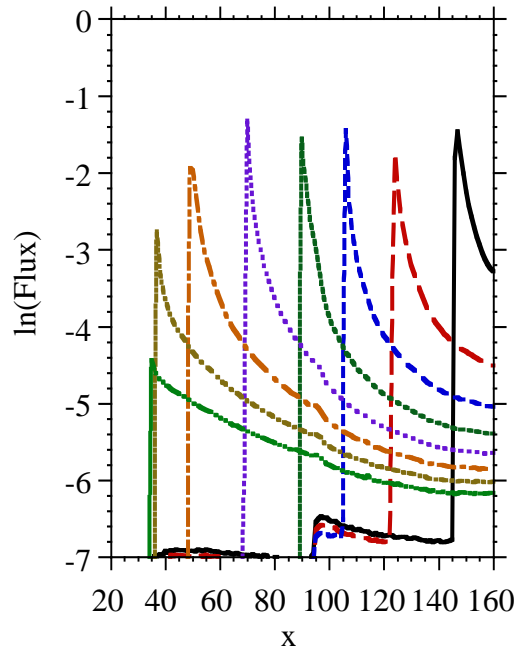


Fig.3 Logarithm of the flux versus radial position at eight equally separated times during the evolution of an avalanche.

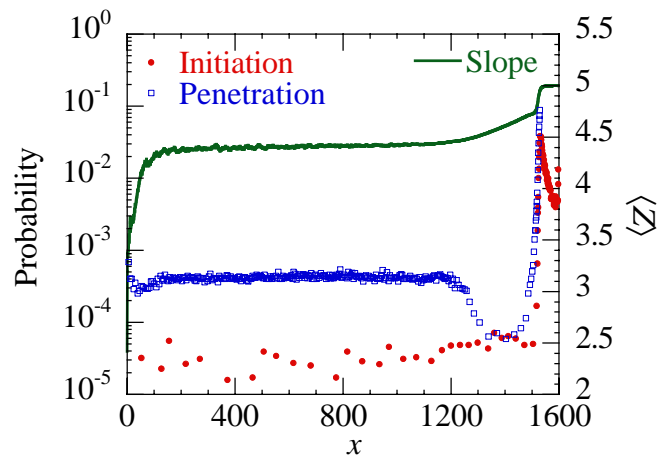


Fig.4 Distribution of initiation points of the avalanches and of the points of maximum inner penetration for  $L = 1600$  system.

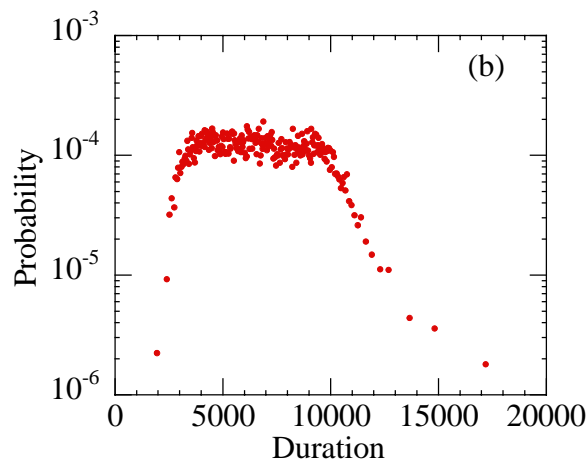
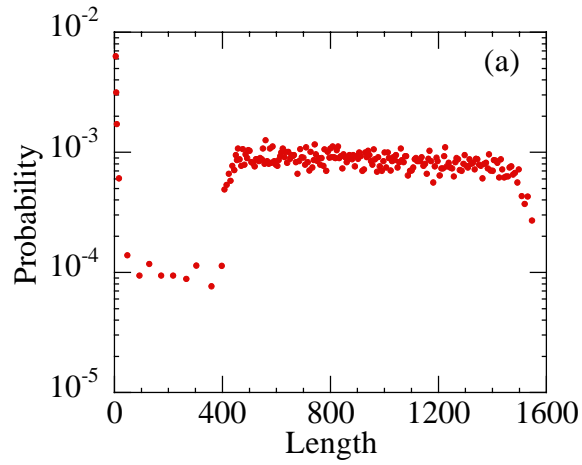


Fig.5 Probability distribution function of the core avalanche length and duration for  $L = 1600$  system.

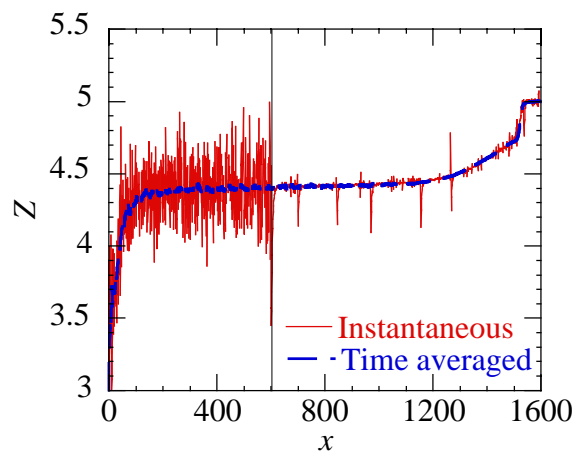


Fig.6 Time-averaged profile with an instantaneous profile of the slope  $Z$  for  $L = 1600$ . The vertical line indicates the position of  $x_m$ .

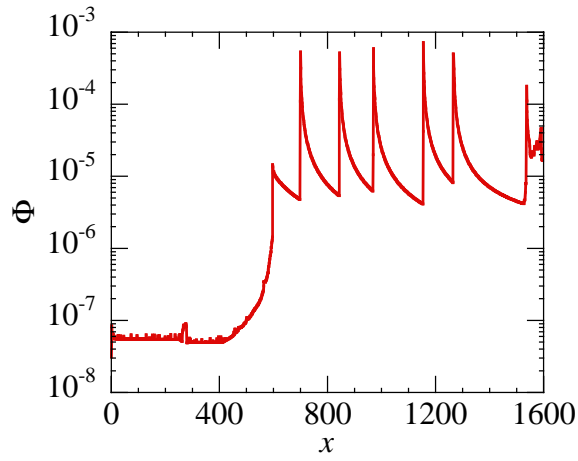


Fig.7 Instantaneous profile of  $\Phi$  for the same time as the instantaneous profile of  $Z$  in Fig. 6.

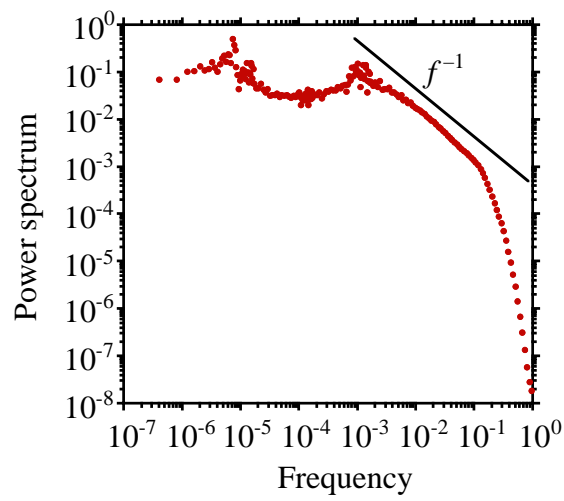


Fig.8 Power spectrum of the flux across  $x = 200$  for  $L = 400$ ,  $p_0 = 5 \times 10^{-5}$ .